Modeling percolation in high-aspect-ratio fiber systems. II. The effect of waviness on the percolation onset

L. Berhan[1],[*] and A. M. Sastry[2]

[1]*Department of Mechanical, Industrial and Manufacturing Engineering, University of Toledo, Toledo, Ohio 43606-3390, USA*
[2]*Department of Mechanical, Biomedical and Materials Science and Engineering, University of Michigan,
Ann Arbor, Michigan 48109-2125, USA*

The onset of electrical percolation in nanotube-reinforced composites is often modeled by considering the geometric percolation of a system of penetrable, straight, rigid, capped cylinders, or spherocylinders, despite the fact that embedded nanotubes are not straight and do not penetrate one another. In Part I of this work we investigated the applicability of the soft-core model to the present problem, and concluded that the hard-core approach is more appropriate for modeling electrical percolation onset in nanotube-reinforced composites and other high-aspect-ratio fiber systems. In Part II, we investigate the effect of fiber waviness on percolation onset. Previously, we studied extensively the effect of joint morphology and waviness in two-dimensional nanotube networks. In this work, we present the results of Monte Carlo simulations studying the effect of waviness on the percolation threshold of randomly oriented fibers in three dimensions. The excluded volumes of fibers were found numerically, and relationships between these and percolation thresholds for two different fiber morphologies were found. We build on the work of Part I, and extend the results of our soft-core, wavy fiber simulations to develop an analytical solution using the more relevant hard-core model. Our results show that for high-aspect-ratio fibers, the generally accepted inverse proportionality between percolation threshold and excluded volume holds, independent of fiber waviness. This suggests that, given an expression for excluded volume, an analytical solution can be derived to identify the percolation threshold of a system of high-aspect-ratio fibers, including nanotube-reinforced composites. Further, we show that for high aspect ratios, the percolation threshold of the wavy fiber networks is directly proportional to the analytical straight fiber solution and that the constant of proportionality is a function of the nanotube waviness only. Thus the onset of percolation can be adequately modeled by applying a factor based on fiber geometry to the analytical straight fiber solution.

I. INTRODUCTION

Electrical conductivity in nanotube-reinforced polymers follows a classic percolationlike behavior [1–11]. Thus the study of percolation in these materials is of high interest and is motivated by the potential for their use as electrically and/or thermally conductive systems with an extremely low concentration of nanotubes. The classic percolation models for sticks in three dimensions are often applied to the prediction of percolation onset in nanotube-reinforced composites [8,12,13]. In these numerical and analytical studies nanotubes are modeled as penetrable, straight, rigid, capped cylinders, or spherocylinders. There are two significant differences between this model and the physical system: nanotubes embedded in a polymer matrix do not penetrate each other, and they are typically not straight.

In Part I we investigated the applicability of the soft-core model to nanotube-reinforced composites by comparing numerical results of simulations using both soft-core and hard-core approaches and concluded that the hard-core model is more suitable for modeling electrical percolation onset in these materials. The more convenient soft-core modeling approach is widely used in the literature, however, the error introduced by allowing the fibers to intersect is nonnegligible and is a function of both aspect ratio (length over radius) and tunneling distance.

Solutions for percolation onset in wavy systems are necessary to study percolation in nanotubes, given experimental observations of both structure and mechanical properties. Recent observations have shown that single-walled carbon nanotubes (SWCNTs) embedded in polymer matrices are generally curved or wavy, rather than straight [14–17]. The effect of fiber waviness on percolation threshold has been studied in two-dimensional (2D) systems [18], and very recently by Dalmas [19] in three-dimensional systems. Previously the existing literature on percolation in three-dimensional (3D) fiber systems considered straight fibers only [20–25]. Though the exact 3D structure of embedded nanotubes remains speculative, the effect of nanotube waviness on the elastic properties of nanotube-reinforced composites has been recently investigated using finite element analysis [26] where a sinusoidal model is used for the embedded nanotubes and an analytical approach [27] in which the nanotubes are assumed to be helical. Both studies showed that the effective modulus decreases significantly with increasing nanotubes waviness. Thus understanding any differences in percolation onset due to fiber waviness, in 3D arrays, appears important both for conductivity and mechanical property prediction.

Recently Dalmas [19] investigated the electrical conductivity of entangled three-dimensional networks of nonstraight fibers. Briefly, the network geometry was generated and the contacts between fibers established by considering nearest-neighbor interactions and allowing fibers to overlap. An

*Corresponding author.

equivalent resistor network was then developed by assigning electrical properties to the fibers and the fiber-fiber contacts. The volume conductivity of the network was then found by integration using finite element software. In this work, we do not allow the fibers to intersect and we use an excluded volume approach to model the percolation of hard-core helical fibers.

We have previously used direct Monte Carlo simulations to determine percolation onset in nonstraight, 2D fiber systems [18]. However, such calculations become prohibitively intensive for 3D arrays. Thus, here, we return to a classic, analytical result by Balberg *et al.* [20] based on the relationship between percolation threshold and excluded volume as the basis for our work in wavy, 3D fiber systems.

Briefly, for a system of like objects, the number of objects per unit volume at percolation, q_p, is inversely proportional to the excluded volume, V_{ex}, of one of the objects, that is

$$q_p \approx \frac{1}{V_{ex}}. \tag{1}$$

It has been shown using a cluster expansion method and Monte Carlo simulations that for soft-core rods the constant of proportionality tends to unity as $R/L \rightarrow 0$. Since nanotubes have very high aspect ratios, a popular approach to predicting the percolation threshold, ϕ_c, in nanotube-reinforced composites is to use the analytical expression

$$\phi_c = \frac{V}{V_{ex}}, \tag{2}$$

where V and V_{ex} are the volume and excluded volume of a straight, rigid, soft-core spherocylinder with the length and radius of the average nanotube or nanotube bundle in the composite.

Since nanotubes within a composite do not penetrate each other, a hard-core model more accurately represents the physical problem. In Part I of the present work, we investigated both approaches and showed that the discrepancy between the results obtained using a soft-core model can be significant, even for high-aspect-ratio fiber systems. We showed through Monte Carlo simulations that the excluded volume rule of Eq. (1) is valid for hard-core spherocylinders as well, and further that the constant of proportionality is one in the slender rod limit. We further proposed an alternate approach to predicting percolation in nanotube-reinforced composites where the embedded nanotubes are straight, i.e.,

$$\phi_c = \frac{(1+s)V_{core}}{V_{ex}}. \tag{3}$$

In the above expression, V_{ex} is the excluded volume of the hard-core spherocylinder with the dimensions of the hard core the same as the average nanotube, and a soft shell thickness equal to half the tunneling distance. The volume of the hard core, V_{core}, is the volume of the physical nanotube. The constant of proportionality $(1+s)$ was determined numerically using Monte Carlo simulations. We established that for high aspect ratios $(L/R > 400)$ the constant of proportionality $(1+s)$ is a function of aspect ratio L/R only. For the hard-

core model, the aspect ratio is taken as the ratio of length L to the outer radius of the soft shell R.

The relationship between percolation threshold and excluded volume of Eq. (3) provides a convenient analytical approach to modeling percolation onset and we use this as the framework for our investigation of the effect of waviness on percolation in nanotube-reinforced composites. We develop models applicable to real nanotubes, i.e., helical or corkscrew arrangements. The specific objectives of the present work are as follows.

(1) To derive expressions for the excluded volume of wavy fibers using Monte Carlo simulations given their geometry.

(2) To find the percolation threshold of systems of wavy fibers randomly oriented in three dimensions using Monte Carlo simulations.

(3) To investigate the validity of the excluded volume rule for systems of nonstraight fibers.

(4) To determine the implications of the results for study of mechanics and transport properties of high-aspect-ratio systems such as nanotube-reinforced polymers, and to comment on the applicability of the straight spherocylinder model to these systems.

In Sec. II, we numerically obtain expressions for the excluded volume of helical fibers of different morphologies. Methodology and results of Monte Carlo simulations to determine the percolation threshold of systems of randomly oriented helical fibers are presented in Sec. III. In Sec. IV these results are discussed in the context of determination of a suitable relationship between percolation threshold and excluded volume for wavy fibers.

II. DETERMINATION OF THE EXCLUDED VOLUME OF HELICAL FIBERS

A. Method

A first step in investigating the effect of waviness on percolation threshold and the validity of the excluded volume rule for systems of wavy fibers is to determine the excluded volume of the wavy fibers. Five different fiber geometries, which we label fibers A, B, C, D, and E, were considered in this study, and are shown in plan and elevation views in Fig. 1. All fibers were modeled with hemispheric caps on each end. A helical model was chosen for fibers B–E with geometry defined by the parametric equations

$$x = a \cos t,$$

$$y = a \sin t,$$

$$z = bt. \tag{4}$$

For fiber B, $a=b$ and $0 \leq t \leq \pi$; for fiber C, $a=b$ and $0 \leq t \leq 2\pi$; for fiber D, $a=b$ and $0 \leq t \leq 4\pi$; and for fiber E, $a =5b$ and $0 \leq t \leq 2\pi$. The running length of any helical fiber minus the end caps is given by

$$L = t\sqrt{a^2 + b^2}. \tag{5}$$

In both the excluded volume simulations and the percolation threshold simulations described later, the centerline of each
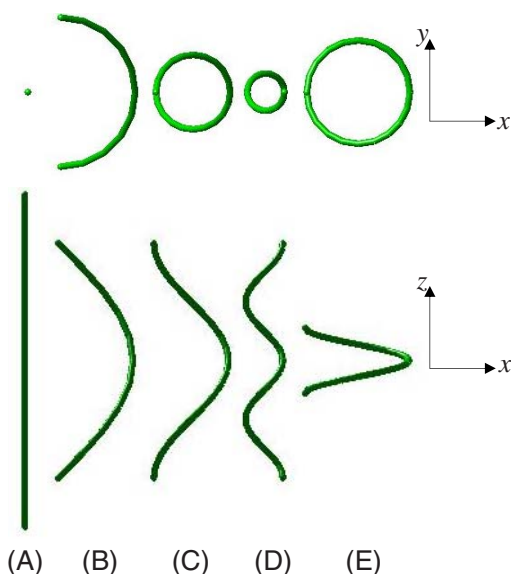
FIG. 1. (Color online) Straight (A) and helical (B, C, D, E) fibers used in the excluded volume study.

helical fiber was modeled using straight line segments. The fibers can thus be considered to be comprised of a series of cylindrical segments, capped with hemispheres on each end of the helix. For convenience we use a soft-core model for our simulations, thus two fibers are considered to intersect if the shortest distance between their centerlines, the distance between their end caps, or the distance between the end cap of one fiber and the centerline of the other fiber is less than or equal to the fiber diameter. Later we will present a method for calculating the excluded volume of hard-core wavy fibers based on the results of the soft-core simulations.

The excluded volumes of the four types of helical fibers were determined numerically, following the procedure outlined by Saar and Manga [28]. For each fiber geometry, the center point of a fiber of running length $L=1$ was placed in the center of a simulation cube with sides of length 2. Next, 10^6 fibers were placed randomly one at a time within the cube, and each checked to determine whether it intersected the original fiber. The number of intersections with the original fiber divided by the number of trials multiplied by the volume of the simulation cube gives the excluded volume of the fiber. For each fiber type, the simulation was performed ten times to determine a mean and standard deviation for V_{ex}. For all fiber types, the excluded volume was found for selected L/R ratios between 20 and 400.

Since the helical fibers are modeled as capped helices, we expect that the excluded volume in each case will be reduced to the excluded volume of a sphere of radius R, $V_{ex_{sphere}}$, in the limit $L=0$. The excluded volume of a sphere of radius R is given by

$$V_{ex_{sphere}} = \frac{32\pi}{3}R^3. \quad (6)$$

We begin with the assumption that the expression for excluded volume in each case will take the same general form

as the excluded volume of the straight capped cylinder, and thus can be expressed as

$$V_{ex} = V_{ex_{sphere}}\left[1 + a_1\left(\frac{L}{R}\right) + a_2\left(\frac{L}{R}\right)^2\right]. \quad (7)$$

We introduce the term $\bar{v}_{ex}$ to represent the excluded volume of a fiber of radius R normalized with the excluded volume of a sphere of radius R such that

$$\bar{v}_{ex} = \frac{V_{ex}}{V_{ex_{sphere}}}. \quad (8)$$

In Part I we established that the hard-core model is more suitable for modeling the onset of electrical percolation, thus we will use the hard-core model for our wavy fiber investigation as well. Since the hard core and the surrounding soft shell can be viewed as capped helices of the same running length and shape with different radii, the excluded volume of a hard-core curly fiber is simply the excluded volume of the core minus that of the impenetrable shell. Thus for the wavy hard-core fiber

$$V_{ex} = V_{ex_{sphere}}\left[(1-t^3) + a_1\left(\frac{L}{R}\right)(1-t^2) + a_2\left(\frac{L}{R}\right)^2(1-t)\right], \quad (9)$$

where t is the ratio of the radius of hard core to the outer radius of the soft shell. The soft-core limit corresponds to a value of $t=0$ while $t=1$ represents the hard-core limit.

The values of the constants in Eq. (9) can be found from simulations to find the excluded volume of soft-core fibers as described above. Once the constants are found, the excluded volume for the hard-core fibers can be easily found from Eq. (9).

B. Results

For each fiber type, $\bar{v}_{ex}$ was plotted against the aspect ratio L/R and the data fit to a second order polynomial with the intercept on the $\bar{v}_{ex}$ axis set to 1. The results are shown in Fig. 2, together with the analytic solution for straight fibers.

Each data point represents the mean value for the ten simulations performed for the given fiber type and aspect ratio, with the error bars indicating plus and minus one standard deviation. The constants a_1 and a_2 [Eq. (7)] for each case are shown in Table I below.

III. NUMERICAL DETERMINATION OF PERCOLATION THRESHOLD: WAVY FIBERS

A. Method

In our simulations for straight fibers performed in Part I, we established that the percolation threshold, q_p, is inversely proportional to the excluded volume for both soft-core and hard-core fiber models and found that q_p followed the general form
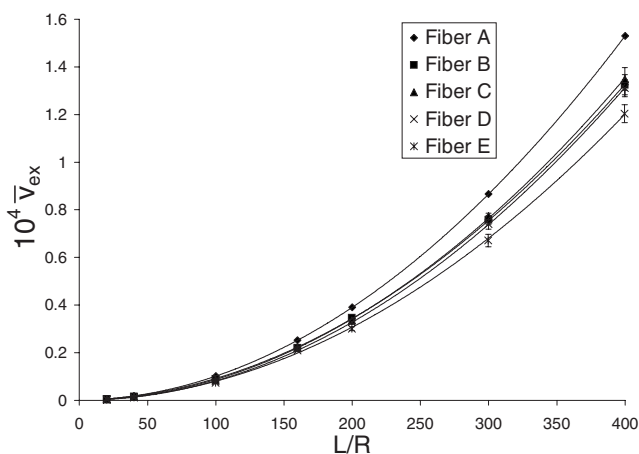
$$q_p = \frac{1+s}{V_{ex}}, \quad (10)$$

where

FIG. 2. Normalized excluded volume $\bar{v}_{\mathrm{ex}}$ vs aspect ratio for fiber types A–E.

$$s = c_1 \left(\frac{R}{L}\right)^{c_2} \qquad (11)$$

for both soft-core and hard-core models. Thus we confirmed that in the slender rod limit (i.e., as $R/L \to 0$) the constant of proportionality is unity for straight fibers.

In order to derive an analytical approach to predicting percolation threshold in wavy fiber systems, we must first investigate whether the excluded volume is valid for wavy fibers. Since the simulations for soft-core fibers are less computationally intensive than those for hard-core fibers, we will establish the relationship between percolation and excluded volume for wavy fibers by considering a soft-core model.

The percolation threshold for soft-core wavy fiber systems of fiber types C and E, respectively, were found following the same approach used for the straight fibers and described in Part I. In the case of fibers of type C, the percolation threshold of systems of fibers of length $L=0.15$ and 0.2, with aspect ratios 20, 30, 40, and 60, were found. For fibers of type E, the percolation threshold was found for systems of fibers of $L=0.2$ and the same values of aspect ratio. One-hundred simulations were performed for each case. The mean number of fibers within the unit cube at percolation, N_c, was found for each aspect ratio and fiber type. Since a simulation cube of unit volume was used, the number of fibers per unit volume at percolation, q_p, is numerically equal to N_c.

In order to investigate the relationship between the percolation threshold and the excluded volume, we use the nu-

TABLE I. Coefficients a_1 and a_2 in Eq. (7) for fibers A–E.

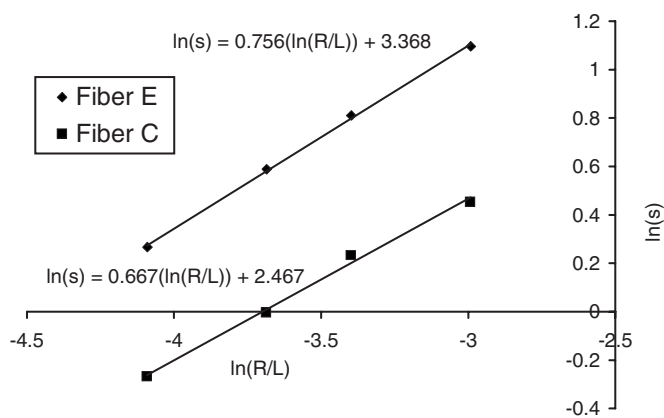| Fiber type	a_1	a_2
A	0.750	0.094
B	1.132	0.080
C	0.374	0.084
D	−0.050	0.082
E	0.646	0.074

FIG. 3. $\ln(s)$ vs $\ln(R/L)$ for fiber types C and E ($L=0.2$).

merical expressions for the excluded volume of the wavy fibers as derived in the previous section. Substituting the values of a_1 and a_2 from Table I into Eq. (7) for fibers C and E, the excluded volume for soft-core fibers of these types can be written as

$$V_{\mathrm{ex}} = \frac{32\pi}{3} R^3 \left[1 + 0.374\left(\frac{L}{R}\right) + 0.082\left(\frac{L}{R}\right)^2 \right] \qquad (12)$$

and

$$V_{\mathrm{ex}} = \frac{32\pi}{3} R^3 \left[1 + 0.646\left(\frac{L}{R}\right) + 0.074\left(\frac{L}{R}\right)^2 \right], \qquad (13)$$

respectively. As in the straight fiber case, the value of s for each aspect ratio was calculated using the mean number of fibers per unit volume at percolation from the simulation results using the expression

$$s = q_p V_{\mathrm{ex}} - 1. \qquad (14)$$

B. Results

The average values of $\ln(s)$ were plotted against $\ln(R/L)$. Figure 3 below shows $\ln(s)$ versus $\ln(R/L)$ for systems of fibers of length $L=0.2$ and fiber types C and E. As in the straight fiber case, $\ln(s)$ was found to vary linearly with $\ln(R/L)$ for both types of wavy fibers considered. Thus the percolation threshold q_p for all cases can be expressed using Eq. (10), with s given by Eq. (11). The values of c_1 and c_2 obtained in each case are given in Table II.

The percolation threshold for fiber C of lengths 0.15 and 0.2 are within 3% of each other for $R/L=0.05$ and differ by less than 1% for $R/L<0.005$, suggesting that the fibers of length $L=0.2$ can be used without loss of accuracy due to scale effects.

TABLE II. Values of c_1 and c_2 for fiber types A, C, and E.

Fiber type	Fiber length	c_1	c_2
A	0.15	5.231	0.569
A	0.20	5.159	0.560
C	0.15	11.156	0.664
C	0.20	11.782	0.667
E	0.20	29.012	0.756

C. Hard-core model

Since the relationship between excluded volume and percolation threshold has been established for the soft-core wavy fibers, we assume that a similar relationship exists for wavy hard-core fibers. While the values of the constants c_1 and c_2 in Eq. (11) are expected to vary with t, we extend the findings of Part I and conjecture that for high aspect ratios, s, and therefore the proportionality constant $(1+s)$, will vary with aspect ratio only and be independent of t.

We therefore propose the use of Eq. (3) as an analytical method for calculating the percolation threshold for high-aspect-ratio wavy fibers using a hard-core modeling approach. In evaluating the expression, the excluded volume is calculated from Eq. (9), V_{core} is the volume of the hard core of the model fiber (i.e., the volume of the nanotube itself), and s is calculated from Eq. (11) using the values of c_1 and c_2 obtained from the soft-core model Monte Carlo simulations.

The radii of single nanotubes and nanotube bundles found in nanotube-reinforced composites range from ~ 0.7 nm to several nanometers. Assuming that the intertube/interbundle spacing required for electron transport (i.e., tunneling distance) is approximately 5 nm or less [14], the range of values of t likely in these materials is 0.2–0.8.

We introduce the quantity $\bar{q}_p$ which serves as a measure of the effect of fiber waviness on percolation threshold.

$$\bar{q}_p = \frac{q_{p(\text{wavy})}}{q_{p(\text{straight})}}, \tag{15}$$

where $q_{p(\text{wavy})}$ is the number of wavy fibers of running length L and aspect ratio L/R per unit volume at percolation, and $q_{p(\text{straight})}$ is the number of straight fibers of the same running length and aspect ratio per unit volume at percolation. Both $q_{p(\text{wavy})}$ and $q_{p(\text{straight})}$ are derived using Eq. (10) with the appropriate values of s and v_{ex}. We define $\bar{v}_{\text{ex}}$ as follows:

$$\bar{v}_{\text{ex}} = \frac{v_{\text{ex(wavy)}}}{v_{\text{ex(straight)}}}. \tag{16}$$

Figure 4 shows $\bar{v}_{\text{ex}}$ versus L/r for the value of $t=0$. Figure 5 is a plot of $\bar{q}_p$ versus L/r for fiber types C and E.

IV. DISCUSSION

For aspect ratios greater than ~ 1000, the value of $\bar{v}_{\text{ex}}$ for a given fiber is independent of aspect ratio as shown in Fig.
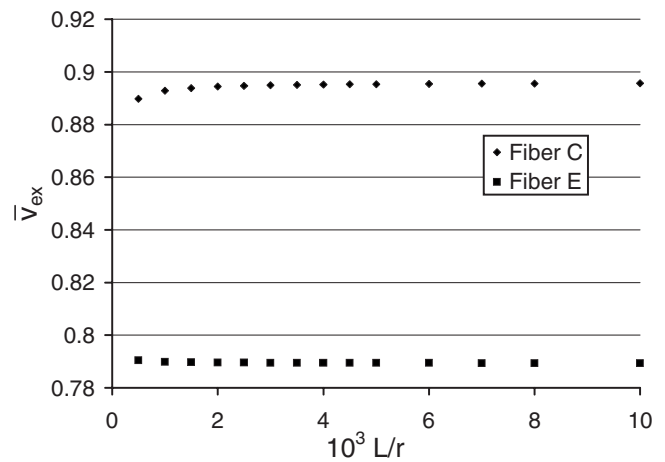

FIG. 4. $\bar{v}_{\text{ex}}$ vs L/r for ($t=0$).

4 which exhibits the quantity $\bar{v}_{\text{ex}}$ for fiber types C and E calculated at $t=0$. Similar plots of $\bar{v}_{\text{ex}}$ versus L/r at the other values of t considered show that for L/r greater than 1000, $\bar{v}_{\text{ex}}$ is also independent of t. Thus at these high aspect ratios, $\bar{v}_{\text{ex}}$ is a constant, α, that depends on fiber geometry only. The values of α for fiber types C and E are 0.79 and 0.89, respectively.
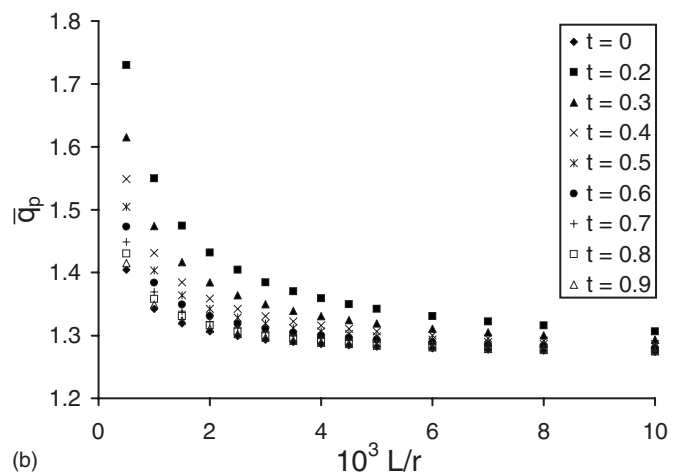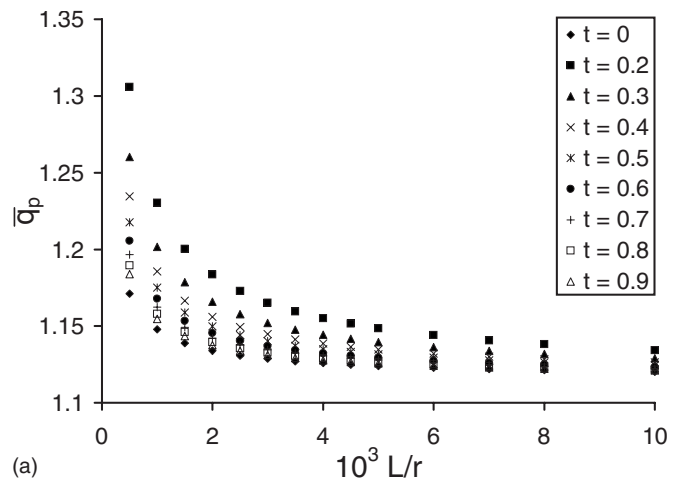

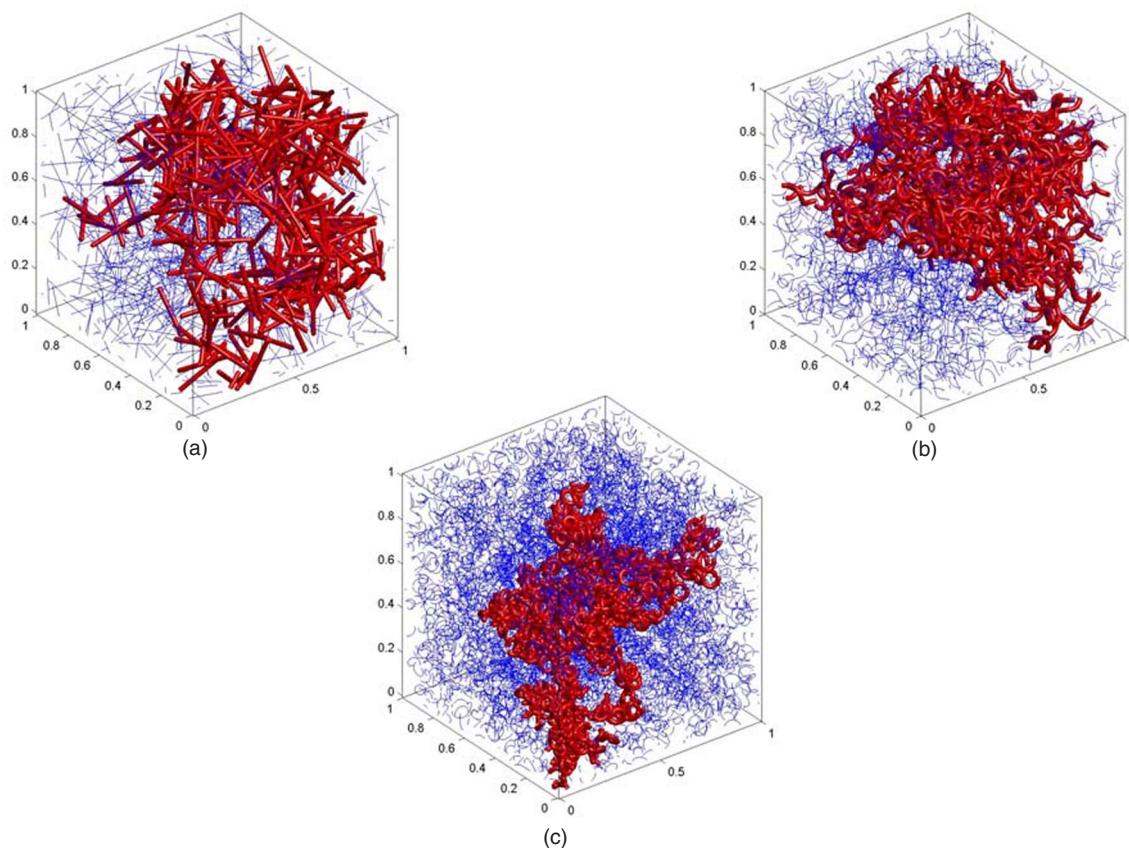FIG. 5. $\bar{q}_p$ vs L/r for fiber types (a) C and (b) E.

FIG. 6. (Color online) Sample networks ($L=0.2$ and aspect ratio$=10$) at percolation for networks of (a) fiber A (straight), (b) fiber C, and (c) fiber E.

As shown in Fig. 5, the effect of fiber waviness on percolation threshold is dependent on both aspect ratio and the ratio of the soft shell to hard-core radii, t, for aspect ratios less than 1000. As the aspect ratio increases, the effect of t decreases and the values of $\bar{q}_p$ converge. This result is in agreement with our simulations for straight fibers presented in Part I and with the findings of Balberg and Binenbaum [21] as discussed in Part I. Thus the number of intersections per fiber B_c [i.e., $(1+s)$ in our simulations] for elongated objects appears to be independent of t as $L/R \rightarrow 0$ regardless of object geometry. Further, for aspect ratios greater than 1000, the magnitudes of $\bar{q}_p$ at all values of t are numerically within 5% of the inverse of the constant α.

Therefore for systems of high-aspect-ratio (i.e., $L/r > 1000$) wavy fibers, including nanotube-reinforced composites

$$\bar{q}_p = \frac{1}{\alpha}, \qquad (17)$$

where α is a parameter that is a function of fiber waviness only. Rewriting Eq. (17), we can express the number of wavy fibers at percolation as

$$q_{p(\text{wavy})} = \frac{q_{p(\text{straight})}}{\alpha}. \qquad (18)$$

Thus the number of wavy fibers per volume at percolation appears to be directly proportional to the number of equiva- lent straight fibers at percolation, with the constant of the proportionality independent of modeling approach and tun- neling distance. For wavy fiber systems of high aspect ratio, the percolation threshold can be expressed by a modified form of Eq. (3),

$$\phi_c = \frac{(1 + s_{(\text{straight})})V_{\text{core}}}{\alpha V_{\text{ex(straight)}}}. \qquad (19)$$

In the above equation, s is calculated using c_1 and c_2 values for an equivalent straight, soft-core fiber, i.e., having the same running length and aspect ratio as the average wavy fiber in the system. $V_{\text{ex(straight)}}$ is the excluded volume of the equivalent straight fiber using a hard-core approach given the fiber radius, aspect ratio, and tunneling distance (from which t can be calculated). As before V_{core} is the volume of the hard core, which is the actual volume of the average fiber in the real system. The only additional simulations required when dealing with high-aspect-ratio wavy fiber systems are those required to determine the aspect ratio, and thus to obtain the value of α.

For aspect ratios less than 1000, the effect of waviness on percolation threshold increases with decreasing aspect ratio and with increasing t. At an aspect ratio of 20, for example, the critical concentration of fibers of types C and E at $t=0$ are 1.46 and 2.09 times the critical number of straight fibers of the same length. This is illustrated in Fig. 6, which shows the fibers (and portions of fibers) present in the unit cube at

percolation for sample networks of fiber types A, C, and E, respectively. All fibers have an aspect ratio $L/r=20$. The actual three-dimensional shapes of the fibers contained in the percolating clusters are shown, with the centerlines of the remaining fibers represented as lines for clarity. For an actual composite this effect is even more pronounced. For example, for an aspect ratio of 20 and $t=0.3$, the critical concentration of fibers of types C and E are $\sim$1.87 and 2.74 times that of a system of equivalent straight fibers.

V. CONCLUSIONS

The percolation threshold of systems comprised of high-aspect-ratio wavy fibers was found to be inversely proportional to the excluded volume of a wavy fiber, and to obey the rule that the constant of proportionality is one in the limit $R/L \rightarrow 0$. The percolation threshold of these systems was also found to be proportional to the percolation threshold for a system of equivalent straight fibers for aspect ratios above 1000, with the constant of proportionality being governed by the fiber waviness only. For the two wavy types C and E considered, this constant of proportionality, $1/\alpha$, was numerically equal to 1.12 and 1.27, respectively.

For systems comprised of highly curved or wavy fibers, an analytical approach can be used to determine the percolation threshold. Although numerical simulations would be required to first determine the excluded volume of the fibers under consideration, these simulations are far less computationally intense than those that would be required to numerically determine the percolation threshold of these networks.

The straight fiber hard-core model is therefore most appropriate when modeling composite materials with straight or very mildly curved fibers of high aspect ratio. If fibers are highly curved or coiled, the discrepancy between models using straight and curved fibers is significant. For short fiber composites, the effect of fiber waviness is predicted to be even more pronounced and inclusion of this effect is critical in predicting percolation threshold.

[1] R. Andrews *et al.*, Macromol. Mater. Eng. **287**, 395 (2002).

[2] J. M. Benoit *et al.*, Synth. Met. **121**, 1215 (2001).

[3] M. J. Biercuk *et al.*, Appl. Phys. Lett. **80**, 2767 (2002).

[4] G. B. Blanchet, C. R. Fincher, and F. Gao, Appl. Phys. Lett. **82**, 1290 (2003).

[5] J. N. Coleman, S. Curran, A. B. Dalton, A. P. Davey, B. McCarthy, W. Blau, and R. C. Barklie, Phys. Rev. B **58**, R7492 (1998).

[6] B. E. Kilbride *et al.*, J. Appl. Phys. **92**, 4024 (2002).

[7] E. Kymakis, I. Alexandou, and G. A. J. Amaratunga, Synth. Met. **127**, 59 (2002).

[8] Z. Ounaies *et al.*, Compos. Sci. Technol. **63**, 1637 (2003).

[9] P. Potschke, T. D. Fornes, and D. R. Paul, Polymer **43**, 3247 (2002).

[10] J. Sandler *et al.*, Polymer **40**, 5967 (1999).

[11] K. Yoshino *et al.*, Fullerene Sci. Technol. **7**, 695 (1999).

[12] M. Foygel, R. D. Morris, D. Anez, S. French, and V. L. Sobolev, Phys. Rev. B **71**, 104201 (2005).

[13] M. Grujicic, G. Cao, and W. N. Roy, J. Mater. Sci. **39**, 4441 (2004).

[14] F. M. Du *et al.*, Macromolecules **37**, 9048 (2004).

[15] J. Loos *et al.*, Ultramicroscopy **104**, 160 (2005).

[16] D. Qian *et al.*, Appl. Phys. Lett. **76**, 2868 (2000).

[17] M. S. P. Shaffer and A. H. Windle, Adv. Mater. (Weinheim, Ger.) **11**, 937 (1999).

[18] Y. B. Yi, L. Berhan, and A. M. Sastry, J. Appl. Phys. **96**, 1318 (2004).

[19] F. Dalmas *et al.*, Acta Mater. **54**, 2923 (2006).

[20] I. Balberg, C. H. Anderson, S. Alexander, and N. Wagner, Phys. Rev. B **30**, 3933 (1984).

[21] I. Balberg and N. Binenbaum, Phys. Rev. A **35**, 5174 (1987).

[22] I. Balberg, N. Binenbaum, and N. Wagner, Phys. Rev. Lett. **52**, 1465 (1984).

[23] A. L. R. Bug, S. A. Safran, and I. Webman, Phys. Rev. Lett. **54**, 1412 (1985).

[24] Z. Neda, R. Florian, and Y. Brechet, Phys. Rev. E **59**, 3717 (1999).

[25] A. A. Ogale and S. F. Wang, Compos. Sci. Technol. **46**, 379 (1993).

[26] F. T. Fisher, R. D. Bradshaw, and L. C. Brinson, Appl. Phys. Lett. **80**, 4647 (2002).

[27] D. L. Shi *et al.*, J. Eng. Mater. Technol. **126**, 250 (2004).

[28] M. O. Saar and M. Manga, Phys. Rev. E **65**, 056131 (2002).